ARTICLE

Infrared Photodissociation Spectroscopy of $Ti^+(CO_2)_2Ar$ and $Ti^+(CO_2)_n$ ($n=3-7$) Complexes[†]

Xiao-peng Xing[a], Guan-jun Wang[b*], Cai-xia Wang[b], Ming-fei Zhou[b]

a. Department of Chemistry, Tongji University, Shanghai 200092, China
b. Department of Chemistry, Shanghai Key Laboratory of Molecular Catalysts and Innovative Materials, Fudan University, Shanghai 200433, China

$Ti^+(CO_2)_2Ar$ and $Ti^+(CO_2)_n$ ($n=3-7$) complexes are produced by laser vaporization in a pulsed supersonic expansion. The ion complexes of interest are each mass-selected in a time-of-flight spectrometer, and studied with infrared photodissociation spectroscopy. For each complex, a sharp band in the CO stretching frequency region is observed, which confirms the formation of the $OTi^+CO(CO_2)_{n-1}$ oxide-carbonyl species. Small $OTi^+CO(CO_2)_{n-1}$ complexes ($n\leq5$) exhibit CO stretching and antisymmetric CO_2 stretching vibrational bands that are blue-shifted from those of free CO and CO_2. The experimental observations indicate that the coordination number of CO and CO_2 molecules around TiO^+ is five. Evidence is also observed for the presence of another electrostatic bonding $Ti^+(CO_2)_2$ structural isomer for the $Ti^+(CO_2)_2Ar$ complex, which is characterized to have a bent $OCO-Ti^+-OCO$ structure stabilized by argon coordination.

Key words: Infrared photodissociation spectroscopy, Carbon dioxide complex, Titanium, Insertion reaction, Density functional calculation

I. INTRODUCTION

The interactions of transition metal centers with CO_2 serve as the simplest model in understanding the intrinsic mechanism of catalytic CO_2 activation processes. The reactions of atomic transition metal cations with carbon dioxide have been intensively studied both experimentally and theoretically [1−14]. Gas phase kinetic studies show that early transition metal cations are able to activate CO_2 in forming metal monoxide cation and CO, whereas the other transition metal cations form adducts with CO_2 [1]. The geometric structures and binding energies of the transition metal cation-carbon dioxide adducts were determined via photon- or collision induced dissociation in gas phase [15−20]. The coordination of carbon dioxide to first transition row metal cations and the insertion reaction of the metal into one CO bond of carbon dioxide were theoretically studied [21]. It was found that the linear end-on M^+-OCO structure is the most favorable coordination for CO_2, due to the electrostatic nature of the bonding. For the early transition metals (Sc^+, Ti^+, and V^+), the insertion reaction is exothermic and the inserted OM^+CO structure is more stable

than the linear M^+-OCO isomer, because of the very strong MO^+ bond that is formed. The electronic photodissociation spectrum of $V^+(CO_2)$ was obtained and the frequencies of vibrational modes were determined from the assigned spectrum [22, 23]. The IR spectra of several $M^+(CO_2)_n$ complexes containing vanadium, iron, nickel, magnesium, aluminum, and silicon have been obtained via mass-selected infrared photodissociation spectroscopy [24−30]. The late transition metal ions were found to bind exclusively to CO_2 molecules in the end-on M^+-OCO configuration predicted by theory. Spectra for $Ni^+(CO_2)_n$ and $V^+(CO_2)_n$ complexes provided evidence for an intracluster insertion reaction that produces a metal oxide-carbonyl species [24, 26]. Such intracluster insertion reaction appears only in the larger clusters.

In this work, the infrared photodissociation spectra of mass selected $Ti^+(CO_2)_2Ar$ and $Ti^+(CO_2)_n$ ($n=3-7$) complexes are reported. $OTi^+CO(CO_2)_{n-1}$ oxide-carbonyl structures are the dominated species observed. Besides the $OTi^+CO(CO_2)$ oxide-carbonyl species, another electrostatic bonding $Ti^+(CO_2)_2$ complex isomer is also formed for the $Ti^+(CO_2)_2Ar$ complex.

II. EXPERIMENTAL AND COMPUTATIONAL METHODS

The infrared photodissociation spectra of the complexes were measured using a collinear tandem time-of-

---

flight mass spectrometer. The experimental apparatus has been described in detail previously [31, 32]. The cation complexes were produced in a laser vaporization supersonic ion source. The 1064 nm fundamental of a Nd:YAG laser (Continuum, Minilite II, 10 Hz repetition rate and 6 ns pulse width) was used to vaporize a rotating titanium metal target. The complexes were produced from the laser vaporization process in expansions of helium/argon gas mixture seeded with 4%−6% CO_2 using a pulsed valve (General Valve, Series 9) at 1.0−1.2 MPa backing pressure. After free expansion, the cations were skimmed and analyzed using a Wiley-McLaren time-of-flight mass spectrometer. The ions of interest were mass selected and decelerated into the extraction region of a second collinear time-of-flight mass spectrometer, where they were dissociated by a tunable IR laser. The fragment and parent cations were reaccelerated and mass analyzed by the second time-of-flight mass spectrometer.

The infrared source used in this work is generated by an KTP/KTA optical parametric oscillator/amplifier system (OPO/OPA, Laser Vision) pumped by a Continuum Powerlite 8000 Nd:YAG laser, which is tunable from 2000 cm^{-1} to 5000 cm^{-1}, producing about 1.0−2.0 mJ/pulse in the range of 2000−2500 cm^{-1}. The infrared laser is loosely focused by a CaF_2 lens. The wavenumber of the OPO laser is calibrated using CO absorptions. The IR beam path is purged with nitrogen to minimize absorptions by air. Fragment ions and undissociated parent ions are detected by a dual micro-channel plate detector. The ion signal is amplified, collected on a gated integrator, and averaged with a LabView based program. The photodissociation spectrum is obtained by monitoring the yield of the fragment ion of interest as a function of the dissociation IR laser wavelength and normalizing to parent ion signal. Typical spectra were recorded by scanning the dissociation laser in steps of 2 cm^{-1} and averaging over 250 laser shots at each wavelength.

Quantum chemistry calculations were performed to determine the molecular structures and to support the assignment of vibrational frequencies of the observed $Ti^+(CO_2)_2Ar$ and $Ti^+(CO_2)_3$ complexes. The calculations were performed with the B3LYP density functional theory (DFT) method, where Becke's three-parameter hybrid functional and the Lee-Yang-Parr correlation functional were used [33, 34]. The aug-cc-PVTZ basis sets were used. The geometries were fully optimized, and the harmonic vibrational frequencies were calculated with analytic second derivatives. CCSD(T) single-point calculations at B3LYP-optimized structures are also performed for selected structures [35]. All these calculations were performed by using the Gaussian 03 program [36]. Theoretical predicted IR spectra were obtained by applying Lorentzian functions with the theoretical harmonic vibrational frequencies scaled by a factor of 0.9775 and a 7 cm^{-1} full width at half-maximum (FWHM).
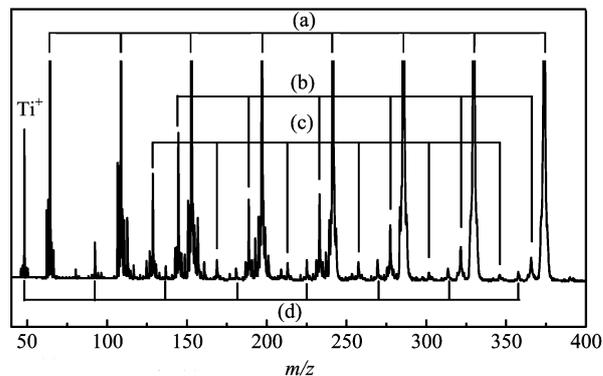
FIG. 1 The mass spectra of the $Ti_xO_y^+(CO_2)_n$ complexes produced by pulsed laser vaporization of a titanium metal target in an expansion of helium seeded by carbon dioxide. (a) $OTi^+(CO_2)_n$ (n=0−7), (b) $Ti_2O_3^+(CO_2)_n$ (n=0−5), (c) $TiO_2^+(CO_2)_n$ (n=0−5), and (d) $Ti^+(CO_2)_n$ (n=0−7).

III. RESULTS AND DISCUSSION

The mass spectrum of the ion complexes produced by the laser vaporization of a titanium metal target in a supersonic expansion of CO_2/H_2 mixture in the m/z range of 40−400 is shown in Fig.1. The spectrum is composed of progressions of mass peaks due to $Ti^+(CO_2)_n$, $TiO^+(CO_2)_n$, $TiO_2^+(CO_2)_n$, and $Ti_2O_3^+(CO_2)_n$ with the $TiO^+(CO_2)_n$ (n=0, 1, 2, ...) peaks dominating the spectrum. The observation of strong $TiO^+(CO_2)_n$, $TiO_2^+(CO_2)_n$, and $Ti_2O_3^+(CO_2)_n$ oxide complexes in the mass spectrum contrasts with previous studies of later transition metals where oxides are not observed [25, 26]. The Ti^+-CO_2 binding energies for the small $Ti^+(CO_2)_n$ complexes ($n \leq 2$) are greater than the infrared photon energies in the CO stretching and antistmmetric CO_2 stretching frequency regions of the complexes; therefore, it is impossible to obtain the infrared spectra of the $Ti(CO_2)_n^+$ complexes with single photon dissociation. The method of rare gas tagging with Ar is employed [37−40]. Photofragmentation proceeds efficiently by elimination of Ar from the $Ti^+(CO_2)_2Ar$ complex. It was found that the larger $Ti(CO_2)_n^+$ complexes with $n \geq 3$ are able to dissociate under IR irradiation through loss of intact CO_2 ligands. The IR spectra of the $Ti^+(CO_2)_2Ar$ and $Ti^+(CO_2)_n$ (n=3−7) complexes are shown in Fig.2 with their band positions listed in Table I.

A. $Ti^+(CO_2)_2Ar$

The experimental spectrum of $Ti^+(CO_2)_2Ar$ (Fig.2(a)) consists of four absorptions at 2184, 2342, 2350, and 2374 cm^{-1} (Table I), indicating that more than one structural isomer is experimentally observed, as any $Ti^+(CO_2)_2Ar$ structure should at most have two

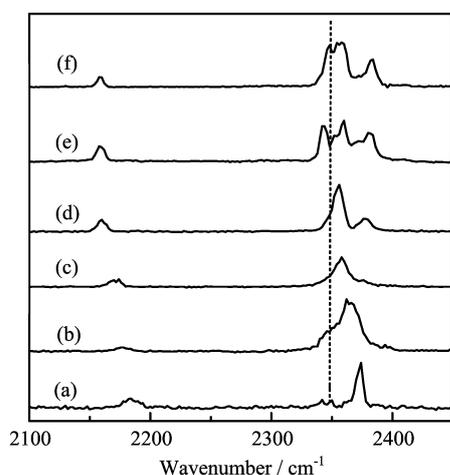FIG. 2 The infrared photodissociation spectra of (a) Ti$^+$(CO$_2$)$_2$Ar complex detected by the elimination of the Ar atom and (b)−(f) Ti$^+$(CO$_2$)$_n$ (n=3−7) complexes detected by the elimination of a CO$_2$ ligand. The dashed line indicates the corresponding frequency of free CO$_2$ molecules.

TABLE I Comparison of the band positions of the Ti$^+$(CO$_2$)$_n$ complexes measured in the present work to those computed by density functional theory at the B3LYP/aug-cc-PVTZ level. The calculated frequencies are scaled by 0.9775, the IR intensities are listed in parentheses in km/mol.

Complex	Experimental	Calculated
Ti$^+$(CO$_2$)$_2$Ar	2342	2366 (1337)
	2350	2383 (917)
OTi$^+$CO(CO$_2$)Ar	2184	2183 (454)
	2374	2383 (1044)
OTi$^+$CO(CO$_2$)$_2$	2176	2162 (442)
	2365	2375 (2000)
		2389 (167)
OTi$^+$CO(CO$_2$)$_3$	2171, 2358, 2375	
OTi$^+$CO(CO$_2$)$_4$	2160, 2355, 2378	
OTi$^+$CO(CO$_2$)$_5$	2159, 2343, 2352,	
	2359, 2372, 2382	

vibrational fundamentals in the CO and antisymmetric CO$_2$ stretching frequency regions. The 2184 cm^{-1} band lies in the region expecting for a CO stretching vibration, which is 41 cm^{-1} blue-shifted from the free CO stretching fundamental at 2143 cm^{-1} [41]. A blue-shifted CO stretching frequency is the signature of nonclassical carbonyls, in which the metal is not able to back donate charge effectively, and CO to metal σ donation and electrostatic polarization play import roles in the metal-CO interaction [42−44]. The remaining three bands above 2300 cm^{-1} can be attributed to the antisymmetric CO$_2$ stretching vibrations.

We assign the 2184 and 2374 cm^{-1} bands to OTi$^+$CO(CO$_2$)Ar, an argon tagged oxide-carbonyl complex. Note that the bare OTi$^+$CO cation was formed via metal cation and carbon dioxide reaction in solid neon matrix. The CO stretching vibration was observed at 2188 cm^{-1} in solid neon, which is 4 cm^{-1} higher than that of OTi$^+$CO(CO$_2$)Ar [45]. The TiO$_2$(CO) complex with CO coordinated to a Ti^{4+} center has an even high CO stretching vibration at 2194 cm^{-1} in solid neon [46]. The 2374 cm^{-1} band is blue-shifted by 25 cm^{-1} from the antisymmetric stretching of free CO$_2$ and can be attributed to the CO$_2$ molecule bound directly to the metal ion. Blue-shifted peaks have been reported in previous investigations on the M$^+$(CO$_2$)$_n$ and MX$_n$(CO$_2$) (X=O, Cl, and Br) complexes [24−29, 45−48], and are rationalized by end-on coordination between an oxygen atom of the CO$_2$ ligand and the metal ion. This blue-shift is very close to that of the V$^+$(CO$_2$)$_n$ complexes [24, 25]. As discussed above, the magnitude of the blue shift correlates with the strength of bonding in the complexes. In general, the transition metal ion complexes exhibit

greater blue shifts than the corresponding main group metal ion complexes, consistent with the stronger bonding in the transition metal complexes.

Besides the strong OTi$^+$CO(CO$_2$) complex absorptions, two weak absorptions at 2342 and 2350 cm^{-1} are also observed in the infrared photodissociation spectrum of mass selected Ti$^+$(CO$_2$)$_2$Ar cations. These two bands are assigned to another structural isomer, the argon tagged Ti$^+$(CO$_2$)$_2$ bis-carbon dioxide complex. For a complex with two CO$_2$ ligands, two vibrational modes are expected in this region, corresponding to in-phase and out of-phase antisymmetric stretching vibrations of the two CO$_2$ ligands. In a linear OCO-Ti$^+$-OCO structure, only the out-of-phase mode is IR-active, while in a bent structure both modes are IR active. The two bands spectrum seen here for the Ti$^+$(CO$_2$)$_2$Ar complex indicates that the two CO$_2$ ligands are arranged in a less symmetric bent configuration.

To validate the experimental assignment, quantum chemical calculations using the density functional theory were performed. The OTi$^+$CO(CO$_2$) complex was predicted to have a ^{2}A$''$ ground state with planar C$_s$ symmetry possessing a nearly linear CO$_2$ ligand with an OCO bond angle of 179.3° (Fig.3). The CO$_2$ ligand is end-on bonded to TiO$^+$ via one O atom with a Ti−O distance of 2.190 Å. The CO fragment coordinates to the titanium center with a Ti−C distance of 2.246 Å. The complex can be viewed as being formed via the ground state of TiO$^+$ ($^2\Delta$) with a CO$_2$ fragment and a CO ligand. Calculations indicate that the argon tagged complex has a non-planar C$_1$ symmetry with the argon atom coordinated to the Ti center approximately perpendicular to the OTi$^+$CO(CO$_2$) molecular plane. The Ti−Ar bond distance is calculated to be 2.702 Å. The geometric parameters of OTi$^+$CO(CO$_2$) change slightly upon argon tagging (Fig.3).
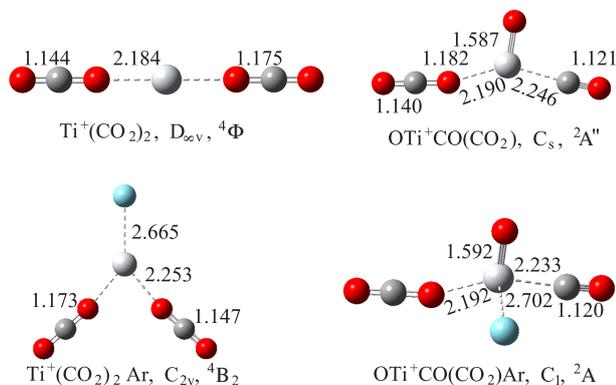
FIG. 3 Optimized structures of the $Ti^+(CO_2)_2$ isomers and their argon tagged complexes. Bond lengths in Å and bond angles in (°).
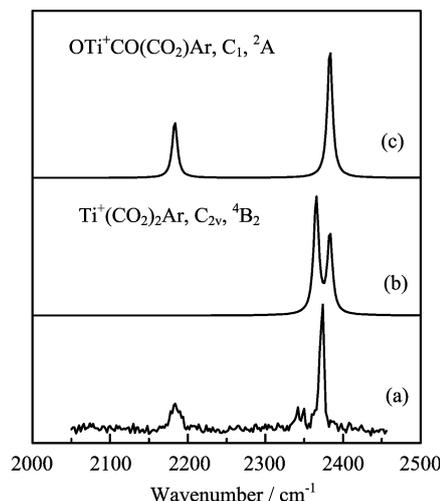

FIG. 4 The experimental and simulated vibrational spectra. (a) The experimental infrared photodissociation spectrum of the $Ti^+(CO_2)_2Ar$ complex detected by the elimination of argon, (b) the simulated spectrum from scaled harmonic frequencies and intensities of the bent $Ti^+(CO_2)_2Ar$ complex, and (c) the simulated spectrum from scaled harmonic frequencies and intensities of the $OTi^+CO(CO_2)Ar$ complex.

Extensive theoretical calculations were also performed on $Ti^+(CO_2)_2$ with and without argon tagging. As has been pointed out in the previous theoretical investigation of first row transition metal ion-carbon dioxide complexes [21], carbon dioxide can behave either as a bidentate ligand (η^2-O,O or η^2-C,O) or as a monodentate ligand (η^1-O or η^1-C) when interacting with neutral metal atoms, but cationic metals are bound to CO_2 electrostatically. Since the leading term is charge-quadrupole and CO_2 has a negative quadrupole moment, the linear η^1-O end-on coordination is the most favorable structure. For the case of two CO_2 complexes, the bonding components are similar to those for the mono-ligand complexes. Therefore, our calculations are performed only on the end-on coordination structures. At the B3LYP level of theory, the most stable structure of $Ti^+(CO_2)_2$ is linear and has a $^4\Phi$ electronic state (Fig.3), derived from the $4s^1d_\pi^1d_\delta^1$ occupation of the metal ion. The $^4\Phi$ state $Ti^+(CO_2)_2$ was predicted to be 28.2 kcal/mol less stable than the $OTi^+CO(CO_2)$ structure. Previous calculations on the Ti^+OCO complex found that the lowest electronic state is also $^4\Phi$, which is 23.9 kcal/mol (B3LYP) or 36.0 kcal/mol (CCSD(T)) less stable than the inserted OTi^+CO isomer with a bent $^2A''$ ground state [21]. Besides the linear structure, we found that a $^4B_2$ state with a bent structure lies 9.7 kcal/mol higher in energy than the $^4\Phi$ ground state. As discussed above, the linear $^4\Phi$ state should have only one IR active mode in the antisymmetric CO_2 stretching region, which does not fit the observed spectrum. In contrast, the higher energy bent $^4B_2$ state was predicted to have two IR active modes, which matches the experimental observation. Further calculations were performed on the argon tagged complexes. We found that the linear $Ti^+(CO_2)_2$ in $^4\Phi$ state cannot form bound complex with argon. In contrast, the bent $^4B_2$ state forms stable complex with argon. The Ti−Ar bond length was predicted to be 2.665 Å. The bent structure is stabilized by 6.3 kcal/mol upon argon atom coordination. The $^4B_2$ $Ti^+(CO_2)_2Ar$ lies only 3.4 kcal/mol

above $Ti^+(CO_2)_2$ ($^4\Phi$)+Ar. CCSD(T) single-point calculations at B3LYP-optimized structures further decrease the energy difference to 2.9 kcal/mol.

The calculated IR spectra of the argon-tagged $OTi^+CO(CO_2)$ and $Ti^+(CO_2)_2$ complexes are compared to the experimental spectrum in Fig.4. The simulated IR spectra support the assignment of the 2184 and 2374 cm^{-1} bands to the $OTi^+CO(CO_2)Ar$ complex, and the 2342 and 2350 cm^{-1} bands to the $Ti^+(CO_2)_2Ar$ complex with a bent structure.

B. $Ti^+(CO_2)_n$ (n=3−7)

We are unable to obtain infrared photodissociation spectra for the $Ti^+(CO_2)_n$ ($n{\geq}3$) complexes with argon tagging, as the $Ti^+(CO_2)_nAr$ ($n{\geq}3$) complexes have identical mass with some other $TiO_x^+(CO_2)_y$ species. Fortunately, these $Ti^+(CO_2)_n$ complexes ($n{\geq}3$) are able to dissociate under IR irradiation through loss of one or more CO_2 ligands. Therefore, the infrared spectra of these complexes are measured by monitoring the loss of one CO_2 ligand. As shown in Fig.2 (b)−(f), each spectrum exhibits a characteristic CO stretching band in the 2150−2180 cm^{-1} region, indicating that the observed species involve the $OTi^+CO(CO_2)_{n-1}$ oxide-carbonyl structures. The CO stretching frequency decreases from 2176 cm^{-1} for the n=3 complex to 2160 cm^{-1} for the n=5 complex, and remains almost unchanged for the n=6 and 7 complexes. In the antisymmetric CO_2 stretching frequency region, only one band centered at 2365 cm^{-1} is observed for the n=3 complex, which can be attributed to the CO_2 stretch-
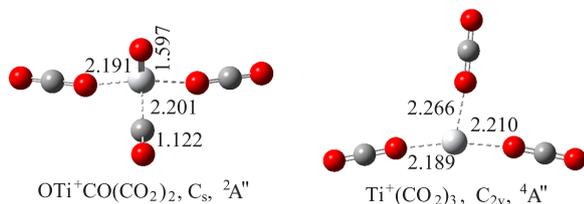
FIG. 5 The optimized structures of the $OTi^+CO(CO_2)_2$ and $Ti^+(CO_2)_3$ complexes. Bond lengths in Å and bond angles in (°).

FIG. 6 The experimental and simulated vibrational spectra. (a) The experimental infrared photodissociation spectrum of the $Ti^+(CO_2)_3$ complex detected by the elimination of a CO_2 ligand, (b) the simulated spectrum from scaled harmonic frequencies and intensities of the $Ti^+(CO_2)_3$ complex, and (c) the simulated spectrum from scaled harmonic frequencies and intensities of the $OTi^+CO(CO_2)_2$ complex.

ing mode of $OTi^+CO(CO_2)_2$. As shown in Fig.5, the $OTi^+CO(CO_2)_2$ complex was predicted to have a $^2A''$ ground state with C_s symmetry. The CO stretching and CO_2 antisymmetric stretching modes were calculated at 2162, 2375, and 2389 cm^{-1}, respectively. The $Ti^+(CO_2)_3$ complex with three η^1-O end-on coordinated CO_2 ligands was predicted to have a $^4A''$ ground state with planar C_s symmetry. This structure was calculated to be 37.2 kcal/mol less stable than the $OTi^+CO(CO_2)_2$ isomer and has two strong antisymmetric CO_2 stretching modes at 2365 and 2373 cm^{-1}. The simulated spectra for the two isomers are compared to the experimental spectrum in Fig.6. The assignment of $OTi^+CO(CO_2)_2$ is obvious. However, the 2365 cm^{-1} band in the experimental spectrum is broad and asymmetric, thus, the coexistence of the $Ti^+(CO_2)_3$ isomer cannot be ruled out.

Two bands at 2358 and 2375 cm^{-1} are observed for the $n=4$ complex, which are blue-shifted by 9 and 26 cm^{-1} from the antisymmetric stretching of free CO_2. These two bands can be attributed to the three CO_2 ligands bound directly to the metal center in $OTi^+CO(CO_2)_3$. The spectrum for the $n=5$ complex involves two sharp well-resolved bands at 2355 and 2378 cm^{-1}, which can be assigned to the CO_2 ligands that are each bound directly to the metal ion via the end-on interaction in $OTi^+CO(CO_2)_4$. The spectrum of the $n=6$ complex is notably different from those of the smaller complexes. Five bands can be resolved in the CO_2 stretching frequency region (Table I). Besides the bands above 2350 cm^{-1} that can be assigned to CO_2 molecules directly bound to the metal ion, a band at 2342 cm^{-1} that is slightly below the antisymmetric stretching of free CO_2 is observed. As discussed previously [24−29], this band arises from the CO_2 molecule in the second coordination sphere, which is bound only to other CO_2 in the first sphere. The spectrum of the $n=7$ complex appears to be very similar to that of the $n=6$ complex, consistent with the presence of both core and surface CO_2 molecules. The first appearance of a strong second sphere CO_2 stretching band at $n=6$ and the fact that the CO stretching frequency remains almost constant after $n=5$ indicate that $OTi^+CO(CO_2)_4$ is a fully coordinated stable complex, and that larger complexes do not add CO_2 ligands that bind directly to the metal center. This establishes that the preferred
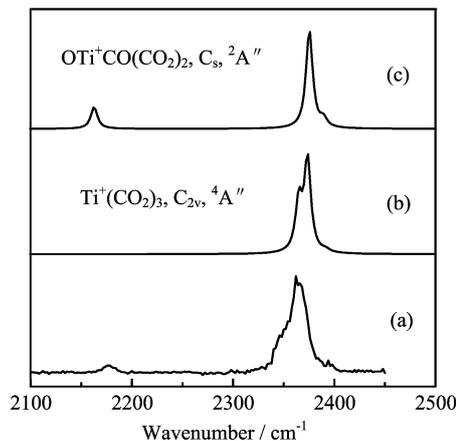
coordination of the TiO^+ cation in these complexes is five. Recent investigation found that the TiO^+ cation is also able to coordinate five CO molecules in forming the $OTi^+(CO)_5$ complex [49].

It is clear from above discussion that the inserted oxide-carbonyl complexes $OTi^+CO(CO_2)_{n-1}$ are formed for all of the $Ti^+(CO_2)_2$Ar and $Ti^+(CO_2)_n$ ($n=3-7$) complexes reported here. The observation of the inserted oxide-carbonyl complexes is consistent with theoretical calculations that the inserted oxide-carbonyl isomers are more stable than the $Ti^+(CO_2)_n$ complexes for $n=2$ and 3. Previous theoretical calculations also found that the inserted structure is more stable than the Ti^+-OCO ion-molecular complex for the $n=1$ complex [21]. This result is somewhat in disagreement with previous reports on $V^+(CO_2)_n$, which observes the inserted structure only in larger complexes that is induced by the effects of solvation [24]. The present experiments also found that the bis-carbon dioxide complex $Ti^+(CO_2)_2$ which is less stable than the oxide-carbonyl isomer is also formed in the $n=2$ complex. The observation of two isomers for the $n=2$ complex suggests that there is an obvious barrier between these two structures.

IV. CONCLUSION

The $Ti^+(CO_2)_2$Ar and $Ti^+(CO_2)_n$ ($n=3-7$) complexes are produced by laser vaporization in a pulsed supersonic expansion, and their infrared photodissociation spectra are reported. Photofragmentation proceeds efficiently by elimination of Ar from the $Ti^+(CO_2)_2$Ar complex and by loss of intact CO_2 molecules from the $Ti^+(CO_2)_n$ ($n=3-7$) complexes. For each complex, a sharp band in the CO stretching frequency

region which is blue-shifted from that of free CO is observed, which confirms the formation of the $OTi^+CO(CO_2)_{n-1}$ oxide-carbonyl species. The spectrum of small $OTi^+CO(CO_2)_{n-1}$ complexes ($n \leq 5$) each exhibits bands in the antisymmetric CO_2 stretching frequency region that are blue-shifted from that of free CO_2. These blue-shifted bands are attributed to the CO_2 ligands directly end-on coordinated to the metal center. The onset of a new band with a frequency slightly lower than that of free CO_2 is first identified at $n=6$, suggesting that four CO_2 molecules comprise the first solvation shell for OTi^+CO in the gas phase. This observation indicates that the coordination number of CO and CO_2 molecules around TiO^+ is five. Besides the bands due to $OTi^+CO(CO_2)$, two additional weak bands in the antisymmetric CO_2 stretching region are observed for the $Ti^+(CO_2)_2Ar$ complex, indicating the presence of another electrostatic bonding $Ti^+(CO_2)_2$ structural isomer. This isomer is characterized to have a bent OCO-Ti^+-OCO structure stabilized by argon coordination.

V. ACKNOWLEDGMENTS

[1] G. K. Koyanagi and D. K. Bohme, J. Phys. Chem. A **110**, 1232 (2006).

[2] J. Herman, J. D. Foutch, and G. E. Davico, J. Phys. Chem. A **111**, 2461 (2007).

[3] M. R. Sievers and P. B. Armentrout, J. Chem. Phys. **102**, 754 (1995).

[4] M. R. Sievers and P. B. Armentrout, Int. J. Mass Spectrom. **185**, 117 (1999).

[5] M. R. Sievers and P. B. Armentrout, Inorg. Chem. **38**, 397 (1999).

[6] M. R. Sievers and P. B. Armentrout, J. Phys. Chem. A **102**, 10754 (1998).

[7] D. M. Han, G. L. Dai, H. Chen, Y. Wang, A. G. Zhong, C. P. Lin, and D. Chen, Int. J. Quantum Chem. **111**, 2898 (2011).

[8] G. L. Dai, Z. Z. Yan, J. Y. Wu, C. F. Wang, H. Chen, and A. G. Zhong, Asian J. Chem. **23**, 3887 (2011).

[9] D. M. Han, G. L. Dai, H. Chen, H. Yan, J. Y. Wu, C. F. Wang, and A. G. Zhong, J. Chem. Sci. **123**, 299 (2011).

[10] G. L. Dai and C. F. Wang, J. Mol. Struct.: THEOCHEM. **909**, 122 (2009).

[11] L. L. Liu, Y. C. Wang, and L. Zhang, Acta Chim. Sin. **68**, 2305 (2010).

[12] Y. C. Wang, X. Y. Yang, Z. Y. Geng, and Z. Y. Liu, Chem. Phys. Lett. **431**, 39 (2006).

[13] S. Di Tommaso, T. Marino, F. Rondinelli, N. Russo, and M. Toscano, J. Chem. Theor. Comput. **3**, 811 (2007).

[14] F. Rondinelli, N. Russo, and M. Toscano, Theor. Chem. Acc. **115**, 434 (2006).

[15] P. B. Armentrout, H. Koizumi, and M. MacKenna, J. Phys. Chem. A **109**, 11365 (2005).

[16] B. L. Tjelta, D. Walter, and P. B. Armentrout, Int. J. Mass Spectrom. **204**, 7 (2001).

[17] D. Bellert, T. Buthelezi, and P. J. Brucat, Chem. Phys. Lett. **290**, 316 (1998).

[18] D. E. Lessen, R. L. Asher, and P. J. Brucat, J. Chem. Phys. **95**, 1414 (1991).

[19] R. L. Asher, D. Bellert, T. Buthelezi, and P. J. Brucat, Chem. Phys. Lett. **227**, 623 (1994).

[20] J. Schwarz and H. Schwarz, Organometallics **13**, 1518 (1994).

[21] M. Sodupe, V. Branchadell, M. Rosi, and C. W. Jr. Bauschlicher, J. Phys. Chem. A **101**, 7854 (1997).

[22] M. Citir and R. B. Metz, J. Chem. Phys. **128**, 024307 (2008).

[23] M. Citir, G. Altinay, and R. B. Metz, J. Phys. Chem. A **110**, 5051 (2006).

[24] N. R. Walker, R. S. Walters, and M. A. Duncan, J. Chem. Phys. **120**, 10037 (2004).

[25] G. Gregoire and M. A. Duncan, J. Chem. Phys. **117**, 2120 (2002).

[26] N. R. Walker, R. S. Walters, G. A. Grieves, and M. A. Duncan, J. Chem. Phys. **121**, 10498 (2004).

[27] G. Gregoire, N. R. Brinkmann, D. van Heijnsbergen, H. F. Schaefer, and M. A. Duncan, J. Phys. Chem. A **107**, 218 (2003).

[28] R. S. Walters, N. R. Brinkmann, H. F. Schaefer, and M. A. Duncan, J. Phys. Chem. A **107**, 7396 (2003).

[29] N. R. Walker, G. A. Grieves, R. S. Walters, and M. A. Duncan, Chem. Phys. Lett. **380**, 230 (2003).

[30] G. Gregoire, J. Velasquez, and M. A. Duncan, Chem. Phys. Lett. **349**, 451 (2001).

[31] G. J. Wang, C. X. Chi, J. M. Cui, X. P. Xing, and M. F. Zhou, J. Phys. Chem. A **116**, 2484 (2012).

[32] G. J. Wang, C. X. Chi, X. P. Xing, C. F. Ding, and M. F. Zhou, Sci. China Chem. **56**, (2013). doi: 10.1007/s11426-013-4979-5.

[33] A. D. Becke, J. Chem. Phys. **98**, 5648 (1993).

[34] C. T. Lee, W. T. Yang, and R. G. Parr, Phys. Rev. B **37**, 785 (1988).

[35] J. A. Pople, M. Head-Gordon, and K. Raghavachari, J. Chem. Phys. **87**, 5968 (1987).

[36] M. J. Frisch, G. W. Trucks, H. B. Schlegel, G. E. Scuseria, M. A. Robb, J. R. Cheeseman, G. Scalmani, V. Barone, B. Mennucci, G. A. Petersson, H. Nakatsuji, M. Caricato, X. Li, H. P. Hratchian, A. F. Izmaylov, J. Bloino, G. Zheng, J. L. Sonnenberg, M. Hada, M. Ehara, K. Toyota, R. Fukuda, J. Hasegawa, M. Ishida, T. Nakajima, Y. Honda, O. Kitao, H. Nakai, T. Vreven, J. A. Jr. Montgomery, J. E. Peralta, F. Ogliaro, M. Bearpark, J. J. Heyd, E. Brothers, K. N. Kudin, V. N. Staroverov, R. Kobayashi, J. Normand, K. Raghavachari, A. Rendell, J. C. Burant, S. S. Iyengar, J. Tomasi, M. Cossi, N. Rega, N. J. Millam, M. Klene, J. E. Knox, J. B. Cross, V. Bakken, C. Adamo, J. Jaramillo, R. Gomperts, R. E. Stratmann, O. Yazyev, A. J. Austin, R. Cammi, C. Pomelli, J. W. Ochterski,

R. L. Martin, K. Morokuma, V. G. Zakrzewski, G. A. Voth, P. Salvador, J. J. Dannenberg, S. Dapprich, A. D. Daniels, Ä. O. Farkas, J. B. Foresman, J. V. Ortiz, J. Cioslowski, and D. J. Fox, *Gaussian 09, Revision A02*, Pittsburgh, PA: Gaussian, Inc., (2009).

[37] M. A. Duncan, Int. Rev. Phys. Chem. **22**, 407 (2003).

[38] M. Okumura, L. I. Yeh, J. D. Myers, and Y. T. Lee, J. Phys. Chem. **94**, 3416 (1990).

[39] E. J. Bieske and O. Dopfer, Chem. Rev. **100**, 3963 (2000).

[40] W. H. Robertson and M. A. Johnson, Annu. Rev. Phys. Chem. **54**, 173 (2003).

[41] K. P. Huber and G. Herzberg, *Molecular Spectra and Molecular Structure IV. Constants of Diatomic Molecules*, New York: Van Nostrand Reinhold Co., (1979).

[42] M. F. Zhou, L. Andrews, and C. W. Bauschlicher, Chem. Rev. **101**, 1931 (2001).

[43] A. S. Goldman and K. Krogh-Jespersen, J. Am. Chem. Soc. **118**, 12159 (1996).

[44] A. J. Lupinetti, G. Frenking, and S. H. Strauss, Angew. Chem. Int. Ed. **37**, 2113 (1998).

[45] M. F. Zhou and L. Andrews, J. Phys. Chem. A **103**, 2066 (1999).

[46] J. Zhuang, Z. H. Li, K. N. Fan, and M. F. Zhou, J. Phys. Chem. A **116**, 3388 (2012).

[47] M. F. Zhou, Z. J. Zhou, J. Zhuang, Z. H. Li, K. N. Fan, Y. Y. Zhao, and X. M. Zheng, J. Phys. Chem. A **115**, 14361 (2011).

[48] M. F. Zhou, L. N. Zhang, M. H. Chen, Q. K. Zheng, and Q. Z. Qin, J. Phys. Chem. A **104**, 10159 (2000).

[49] X. J. Zhou, J. M. Cui, Z. H. Li, G. J. Wang, Z. P. Liu, and M. F. Zhou, J. Phys. Chem. A **117**, 1514 (2013).